



ISSN: 0067-2904

Improving the Performance of Titanium Oxide Nanocomposites as NO₂ Gas Sensors for Optimum Sensitivity

Ameer A. Nemea*, Basim I. Al-Abdaly

Department of Chemistry, College of Sciences, University of Baghdad, Baghdad, Iraq

Received: 23/12/2022 Accepted: 1/4/2023 Published: 30/3/2024

Abstract

In this study, we investigate the performance improvement of titanium oxide (TiO₂) nanocomposites as NO₂ gas sensors for optimum sensitivity. The TiO₂ nanocomposites were synthesized using a solvothermal method and were modified with different dopants and additives to enhance their sensing properties. The sensing performance of the TiO₂ nanocomposites was evaluated in terms of sensitivity, selectivity, response time, and recovery time. The synthesized nanocomposites were successfully characterized using AFM, FTIR, SEM-EDX and XRD techniques. The results showed that the addition of additives such as TiO₂/GO, TiO₂-Ag/GO and TiO₂-Al₂O₃/GO: TiO₂/GO significantly improved the sensing properties of the TiO₂ nanocomposites. The Ag-doped TiO₂ nanocomposites exhibited the highest sensitivity towards NO₂ gas with a very low detection limit. The Al₂O₃-doped TiO₂ nanocomposites showed good selectivity towards NO₂ gas compared to other interfering gases and has led to increase in the surface area. In conclusion, the addition of additives and the optimization of the annealing temperature can significantly improve the sensing properties of TiO₂ nanocomposites towards NO₂ gas. The findings of this study can contribute to the development of highly sensitive and selective NO₂ gas sensors for various applications such as environmental monitoring and industrial safety.

Keywords: TiO₂ NPs , gas sensor, nanocomposites, response , recovery time.

تحسين أداء متراكبات أكسيد التيتانيوم النانوية كمتحسس لغاز NO₂ للحصول على حساسية مثلى

أمير عبد الرحيم نعمة* , باسم إبراهيم العبدلي

قسم الكيمياء، كلية العلوم، جامعة بغداد، بغداد، العراق.

الخلاصة

في هذه العمل، تم دراسة تحسين أداء المتراكبات النانوية لـ TiO₂ كمتحسس غازي لغاز NO₂ بغية الوصول للحساسية المثالية. تم تحضير المتراكبات النانوية لـ TiO₂ باستخدام تقنية (solvothermal) وتعديل النتائج من خلال تشويبها أو تطعيمها بمختلف الإضافات لتعزيز صفات التحسس لديها. تم تقييم أداء التحسس لمتراكبات TiO₂ ضمن جوانب الحساسية، زمن الاستجابة وزمن الاسترجاع. وتم تشخيص المتراكبات المختلفة من خلال عدة تقنيات هي AFM، FTIR، SEM-EDX و XRD. أظهرت النتائج ان عملية الإضافات كما في TiO₂-Ag/GO and TiO₂-Al₂O₃/GO قد حسنت بشكل مهم صفات التحسس لمتراكب الـ TiO₂/GO. المتراكب المشوب بـ Ag قد أظهر أعلى حساسية اتجاه غاز الـ NO₂. كما ان المشوب بـ Al₂O₃ قد أظهر قدر

تحسس جيد نحو غاز NO₂ مقارنةً مع غازات أخرى، وهذا يعود إلى أن زيادة المساحة السطحية للمترابك. في نهاية المطاف فإن إضافة مواد للتشويب مع درجة حرارة مثالية للتحضير بالإمكان تحسين صفات التحسس لمترابكات TiO₂ اتجاه NO₂. نتائج هذه الدراسة بإمكانها المساهمة في تطوير الحساسية والانتقائية لمتحسس غاز NO₂ لمختلف التطبيقات كالمراقبة البيئية والامن الصناعي.

1. Introduction

Nanoparticles have gained immense popularity due to their unique properties and high surface area-to-volume ratio, which make them suitable for a wide range of applications.

One of the areas where nanoparticles have shown significant promise is gas sensing. Gas sensors based on nanoparticles offer a wide range of advantages over conventional gas sensors, including high sensitivity, selectivity, and response time, as well as low power consumption and cost [1,2]. In recent years, the development of new synthesis methods has allowed for the production of nanoparticles with precise control over size, shape, and composition, enabling their use in gas sensing applications. Moreover, the integration of nanoparticles with other materials, such as polymers and graphene, has further expanded the range of gas-sensing applications [3]. Nanoparticles-based gas sensors have been developed for detecting a wide range of gases, including carbon monoxide, nitrogen oxides, methane, and hydrogen. The use of nanoparticles has enabled the development of gas sensors with high selectivity and sensitivity, which are crucial for detecting trace amounts of gases in industrial and environmental settings. Additionally, the miniaturization of nanoparticle-based gas sensors has made them suitable for portable and wearable applications, enabling real-time gas sensing in a variety of settings [4, 5]. Titanium dioxide nanoparticles have a high surface area and reactivity, making them effective gas sensors. They can detect various gases, including nitrogen dioxide, carbon monoxide, and volatile organic compounds, with high sensitivity and selectivity. Titanium dioxide nanoparticles can be combined with other composites such as graphene, metal oxides, and polymers to enhance gas sensing performance. These composites can improve sensitivity, selectivity, and stability, making them suitable for various applications, including environmental monitoring, industrial safety, and medical diagnosis. Additionally, the use of these composites can reduce the cost and improve the fabrication process of gas sensors [6-8]. The flow rate of NO₂ gas was (80-100) ppm since the gas concentration was a key component of the sensing process [9]. As reaction and recovery durations are influenced by temperature, several temperatures have been used [10]. The redox interaction between the gas and the surface of the nanocomposites (sensor) was triggered when NO₂ gas was pumped into the detecting chamber [11]. Several studies have been devoted to efforts to raise the sensitivity of sensors [12], therefore there is a technique to boost activity by increasing surface reaction via addition of a substance like alumina Al₂O₃, which has electrical activity and increases surface area simultaneously. Some times by adding a material that has a high electro activity like silver which has the highest electrical conductivity among all metals [14]. The aim of this scientific paper is to investigate the synthesis of composites comprising titanium dioxide nanoparticles and graphene, silver, and aluminum (TiO₂/GO, TiO₂-Ag /GO and TiO₂-Al₂O₃/GO), with the goal of enhancing the physical, chemical, and optical properties of the resulting materials. Through a systematic approach, the study aims to optimize the synthesis parameters and analyze the morphological, structural, and functional characteristics of the composites, which may have potential applications in NO₂ gas sensing.

2. materials and methods

2.1 chemicals

In this study all materials from Sigma-Aldrich, Titanium tetra isopropoxide ($\text{Ti}[\text{OCH}(\text{CH}_3)_2]_4$) and its purity (96%) and Aluminum isopropoxide ($\text{C}_9\text{H}_{21}\text{AlO}_3$) (pure), absolute ethanol $\text{CH}_3\text{CH}_2\text{OH}$ (98%), and graphite (C) (99.99 %) whereas, de-ionized water from local markets.

2.2 Preparation of TiO_2 NPs by solvothermal method

The solvothermal method is a well-established technique for the synthesis of titanium dioxide nanoparticles. In this method, a precursor solution of titanium isopropoxide is prepared in a suitable solvent and a surfactant is added to control the size and shape of the resulting nanoparticles. Using titanium tetra isopropoxide, isopropanol, and distilled water as the starting components, TiO_2 NPs were produced utilizing the solvothermal technique. To generate a white-coloured solution, 10 mL of distilled water was mixed with titanium tetra isopropoxide (TTIP) and isopropanol at a (1:4) molar ratio. The mixture was then agitated for one hour. Following the formation of a clear solution, the solution was put into a Teflon vessel, put in a stainless autoclave, and the temperature was set at 150°C for 18 hours. The autoclave was then cooled to room temperature, the supernatant was removed, and the precipitate was repeatedly washed with distilled water and ethanol [15,16]. For four hours, TiO_2 nanoparticles were dried at 80°C . The powder was then annealed for 4 hours at 500°C .

2.3 Preparation of $\text{TiO}_2\text{-Al}_2\text{O}_3$ NPs by sol-gel method

To prepare solution (A), a mixture of aluminum isopropoxide (1.5 gm) and isopropanol (25 mL) was stirred for 10 minutes. Then, titanium tetra isopropoxide (6 mL) was added to the aluminum isopropoxide solution while stirring for 30 minutes. To prepare solution (B), concentrated HCl (1 mL) was mixed with isopropanol (30 mL) and de-ionized water (10 mL). Solution (A) was slowly added to solution (B) while stirring vigorously for 30 minutes, resulting in a homogeneous solution. The solution was stirred vigorously for 4 hours, forming a sol, which transformed into a gel after 48 hours. The gel was separated by centrifugation for 15 minutes and dried at 100°C for 24 hours to remove any residual water and organic material. Finally, the dried gel was annealed at 500°C for 3 hours to obtain the desired product in the form of nanoparticles [13, 17].

2.4 Preparation the nanocomposites by ultrasonic

To prepare each product, they were mixed with absolute ethanol and subjected to ultrasonic treatment for 20 minutes. Graphene oxide was then added to de-ionized water and subjected to ultrasonic treatment for 30 minutes. The two solutions were combined by stirring vigorously for 20 minutes and then subjected to ultrasonic treatment for 30 minutes. The final products (TiO_2/GO and $\text{TiO}_2\text{-Al}_2\text{O}_3/\text{GO}$) were obtained by centrifugation and drying, with each product having a ratio of 2:8 with respect to graphene oxide.

2.5 Ag- TiO_2 Nanocomposite

After synthesizing titanium oxide nanoparticles using the hydrothermal method, 0.01 g of TiO_2 NPs were mixed with 20 ml of ethanol and stirred for 30 minutes. The mixture was then subjected to ultrasonic waves for 20 minutes. At the same time, silver nanoparticles were prepared using 1M silver nitrate in de-ionized water, which was stirred for 20 minutes at 60°C . A reducing agent, trisodium citrate, was prepared at 10M and added dropwise to the silver nitrate solution at 60°C until the color of the solution turned pale yellow. The solution was then allowed to cool. The silver nanoparticles were gradually added to the TiO_2 NPs dispersed in ethanol by ultrasonic, with stirring. The resulting mixture was subjected to ultrasonic waves for

an additional 30 minutes. Finally, the mixture was dried to obtain the silver-titanium oxide (Ag-TiO₂) nanocomposite.

3. Results and Discussion

3.1 Results

First of all, it is necessary to study the properties of those nanocomposites by using some techniques like AFM, FTIR, SEM-EDX and XRD those concerning the size, morphology and distribution of nanoparticles and nanocomposites.

To make sure the size and shape of the surface of the TiO₂ is Nano-size before preparing the Nano-composites and it was 28.11nm. It was evident from the AFM (2D and 3D) image that the surface morphology was not smooth and had agglomerated particles, which are represented by the white peaks. This aggregation can be caused by the measurement method [15] as following Figure (2):

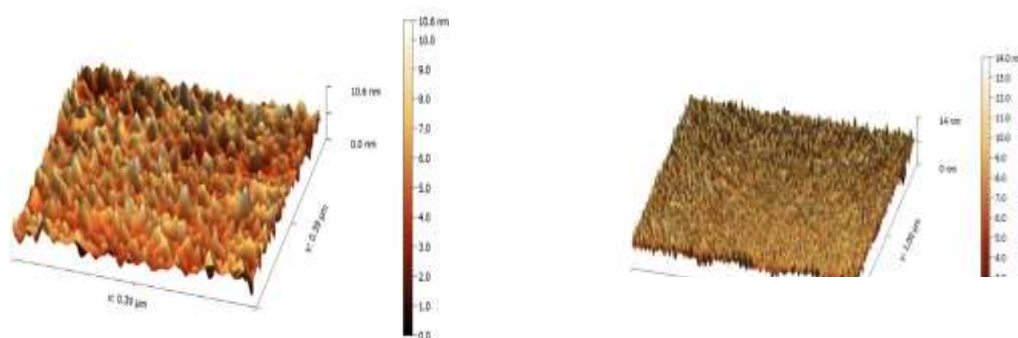


Figure 2: (2D & 3D) AFM images of TiO₂ NPs. Average of diameter 28.11 nm.

TiO₂/ GO nanocomposite

The Figure (3) showed the existence of hydroxyl groups in nanocomposite. There are peaks between (3566.14 - 3292.26 cm⁻¹) are attributed to the stretching vibrations of the (O-H) group which is referred to the significant amount of the H₂O molecules in the interlayer space and surface, and the reaction between the (O-H) groups of TiO₂ / GO, another peak at 1604 cm⁻¹ is ascribed to the (H-O-H) bending mode [13,14]. The peak at 1342.36 cm⁻¹ is referred to the (C-O) stretching, at 1099.35 cm⁻¹ for (H-O-Ti) stretching, and at 613.32 cm⁻¹ for (Ti-O) mode [15,18].

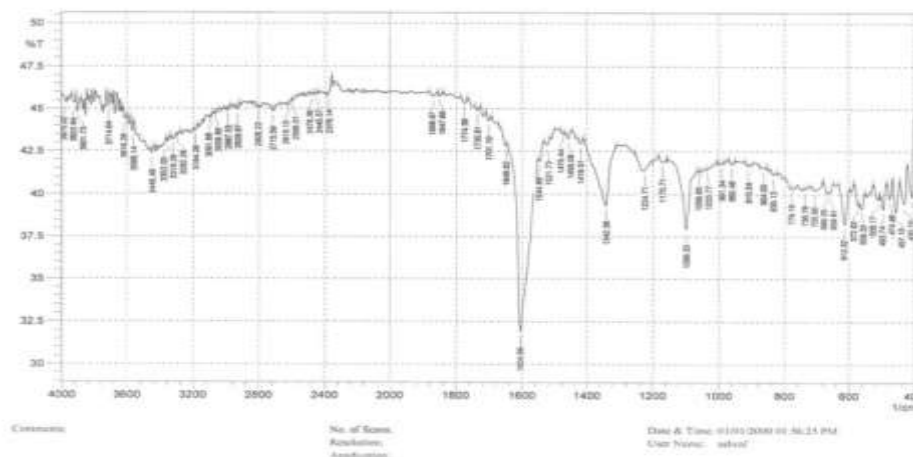


Figure 3: FT-IR spectrum of TiO₂/ GO nanocomposite.

Figure 4 observes the distribution of titanium oxide NPs on the surface of graphene oxide which has shape as sheets that has been shown in the SEM technique, in addition of the components of nanocomposites were (C) 57.4%, (O) 38.5%, and (Ti) 4.1% that have been shown through the EDX technique as in the following images [13,14]:

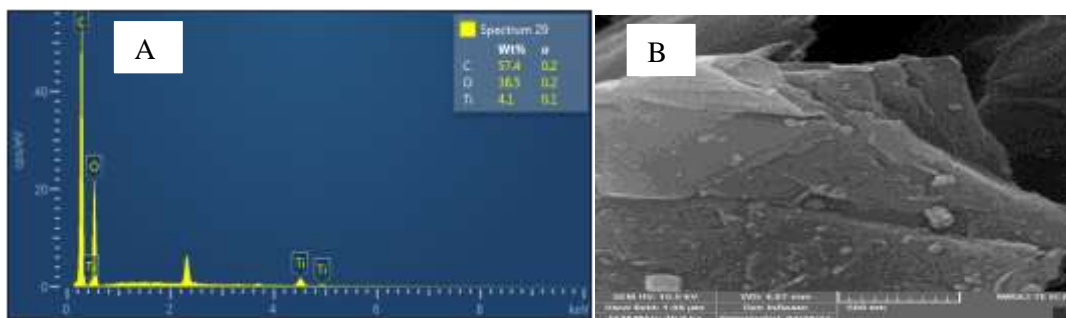


Figure 4: (A) SEM and (B) EDX images of TiO_2 / GO of composition.

Figure 5 illustrates the XRD technique showed a crystalline characteristic and the average crystalline size of the TiO_2 / GO. several diffraction peaks reveal the formation of TiO_2 / GO phase with a good crystallinity. through treatment of the data by the origin pro 8 program and Scherrer equation [13,14] which have been showed the full width at half maximum (FWHM) is (0.50479) , 2 theta (2θ) is 26.4895° and the crystallite size was equal (20 nm), as following pattern [15,18]:

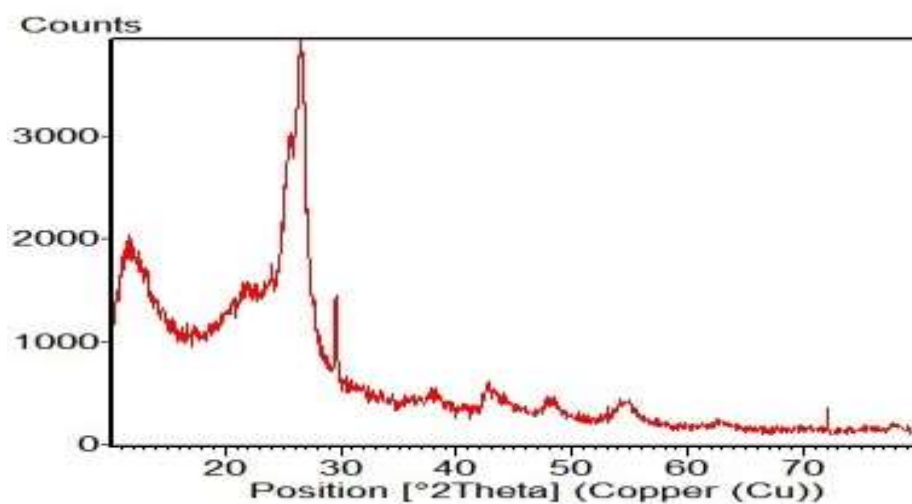


Figure 5: XRD pattern of TiO_2 /GO nanocomposite.

TiO_2 -Ag/GO nanocomposite

Figure 6 the FTIR technique showed different peaks such as (3442.7 cm^{-1} - 3257.55 cm^{-1}) of stretching vibrations of (O-H) group which return to exist an amount of H_2O molecules in the interlayer space and surface [13]. the range (2715.59 cm^{-1} - 2972.10 cm^{-1}) is attributed to stretching of (C-H) of organic residues [14]. there is a peak at 1348.15 cm^{-1} ascribed of ($-\text{NO}_3$) of AgNO_3 , and another peak at 1604 cm^{-1} ascribed to the (H-O-H) bending mode, 1099.35 cm^{-1} for (H-O-Ti) stretching, and 613.32 cm^{-1} (Ti-O) [15,18].

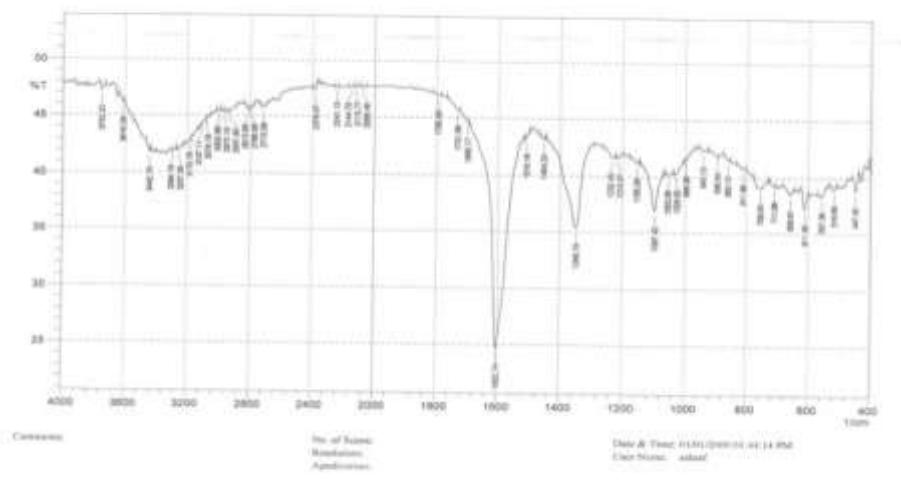


Figure 6: FT-IR spectrum for $\text{TiO}_2\text{-Ag/GO}$ composite.

Figure 7 observes the distribution of $\text{TiO}_2\text{-Ag}$ NPs on the surface of graphene oxide which has shape as sheets that has been shown in the SEM technique, in addition of the components of nanocomposites were (C) 55.38%, (O) 24.89%, (Ti) 2.86% and (Ag) 11.8%, and there are (Na, S and Cl) as the residues from precursors as EDX shows in the following images [13,14]:

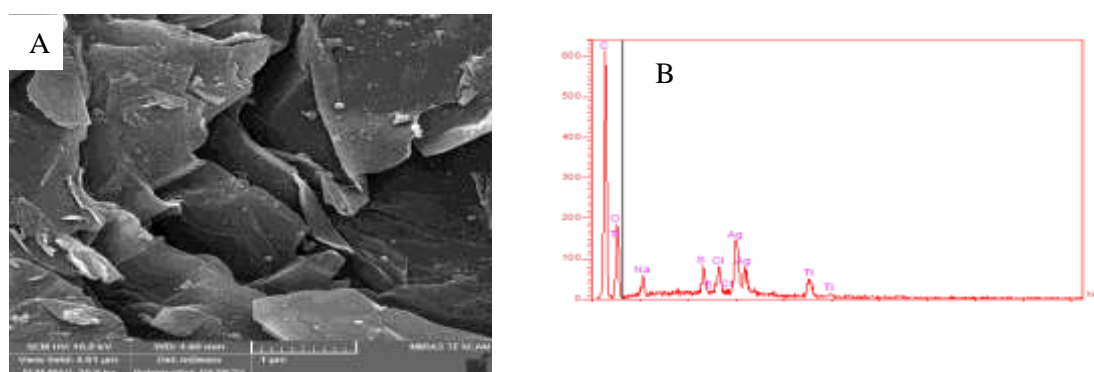


Figure 7: (A) SEM and (B) EDX images of $\text{TiO}_2\text{-Ag/GO}$ of composition.

Figure 8 shows the XRD technique showed a crystalline characteristic and the average crystalline size of the $\text{TiO}_2\text{-Ag/GO}$. several diffraction peaks reveal the formation of $\text{TiO}_2\text{-Ag/GO}$ phase with a good crystallinity. through treatment of the data by the origin pro 8 program and Scherrer equation [13,14], which have been showed the full width at half maximum (FWHM) is (3.86645), 2 theta is 28.57948° and crystallite size equals (14 nm) as following pattern [15,18]:

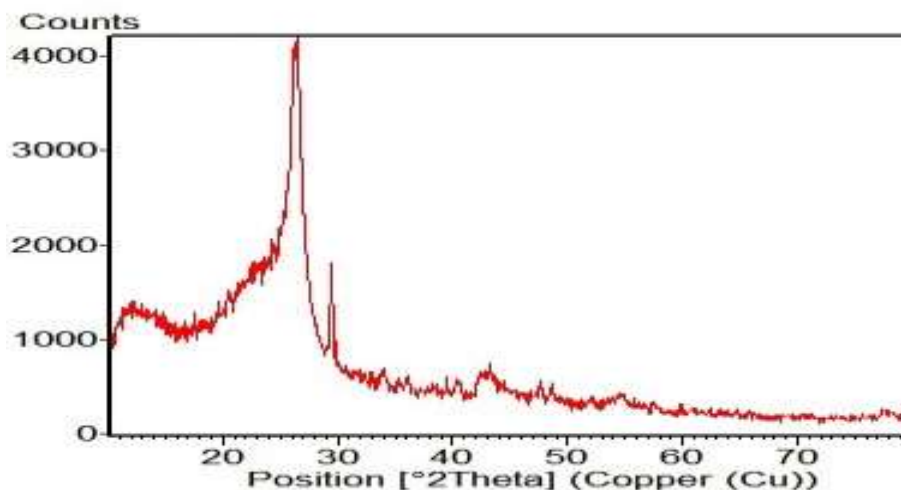


Figure 8: XRD pattern of $\text{TiO}_2\text{-Ag/GO}$ composite.

$\text{TiO}_2\text{-Al}_2\text{O}_3\text{/GO}$ nanocomposite

Figure 9 shows the spectrum showed the existence of hydroxyl groups in samples. There are the peaks at 3434.96 cm^{-1} to 3222.83 cm^{-1} are attributed to the stretching vibrations of (O-H) group which is referred to the significant amount of H_2O molecules in the interlayer space and surface, and the reaction between the (O-H) groups of $\text{TiO}_2 - \text{Al}_2\text{O}_3\text{/GO}$, another peak is 1604 cm^{-1} is ascribed to (H-O-H) bending mode [13,14]. The peak at 1346.22 cm^{-1} is referred to (C-O) stretching, the band at range 1380.94 cm^{-1} to 1473.51 cm^{-1} is indicated the formation of alumina, at 1099.35 cm^{-1} for (H-O-Ti) stretching, and at 765.69 cm^{-1} to 613.32 cm^{-1} (Ti-O-Al). It is noted a weak peak appeared at the range of 2621.08 cm^{-1} to 2933.53 cm^{-1} attributed to the stretching of (C-H) of organic residues [15,18].

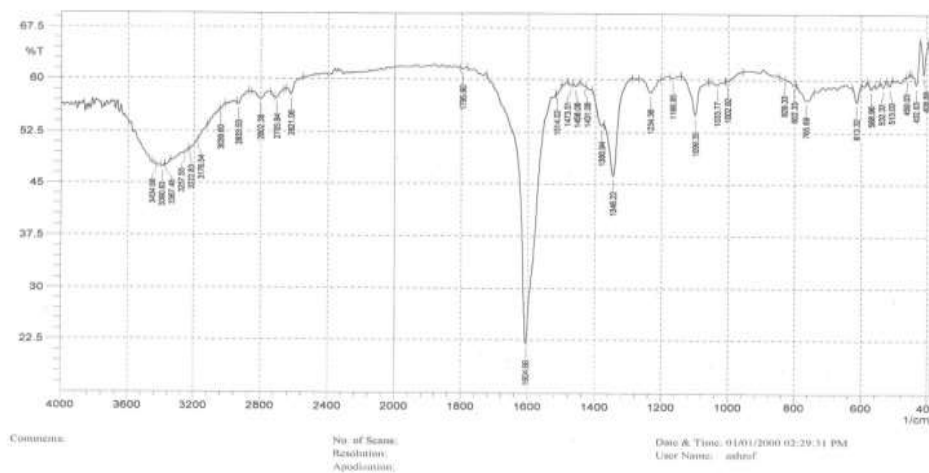


Figure 9: FT-IR spectrum for $\text{TiO}_2\text{-Al}_2\text{O}_3\text{/GO}$ composite.

There was a distribution of $\text{TiO}_2\text{-Al}_2\text{O}_3$ NPs on the surface of graphene oxide as the SEM technique shows, and the components of nanocomposites were (C) 78.4%, (O) 20.8%, (Ti) 0.5%, and (Al) 0.3%, using an EDX technique as shows in the following images as shown in Figure 10[13,14]:

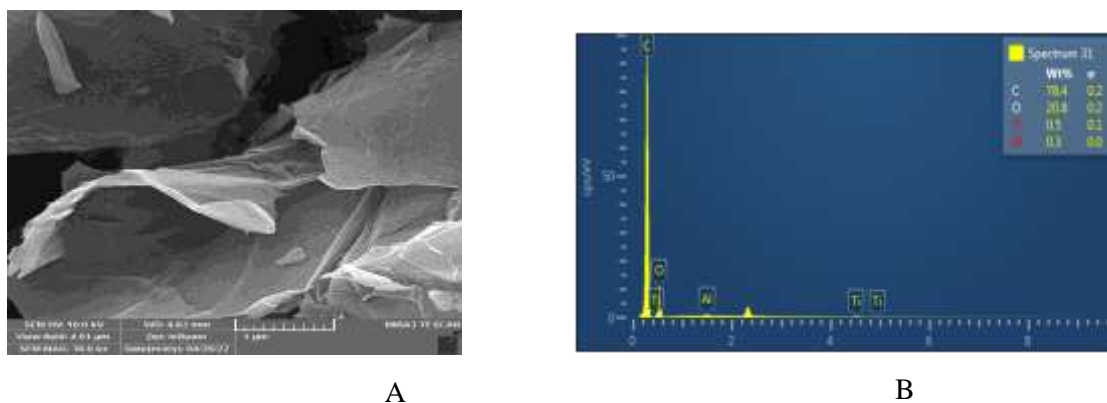


Figure 10: SEM and EDX images of $\text{TiO}_2\text{-Al}_2\text{O}_3 / \text{GO}$ of composition.

The XRD technique showed a crystalline characteristic and the average crystalline size of the $\text{TiO}_2\text{-Al}_2\text{O}_3/\text{GO}$. several diffraction peaks reveal the formation of $\text{TiO}_2\text{-Al}_2\text{O}_3/\text{GO}$ phase with a good crystallinity. through treatment of the data by the origin pro 8 program and Scherrer equation [13,14], which have been showed the full width at half maximum (FWHM) is (3.11302) and 2 theta is 23.77573° and crystallite size equals (7 nm) as showing in Figure 11: [15,18]:

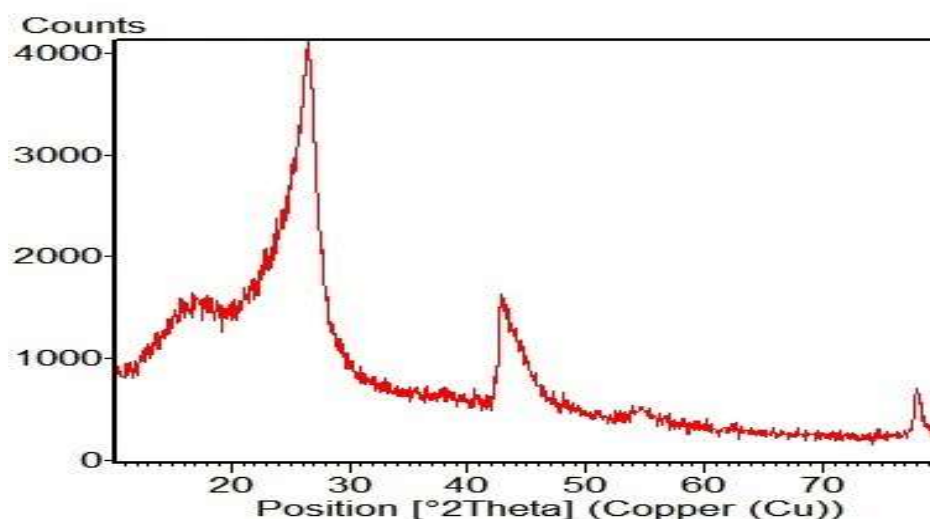


Figure 11: XRD pattern of $\text{TiO}_2\text{-Al}_2\text{O}_3/\text{GO}$ nanocomposite.

3.2 Gas sensing data

In order to present the sensing data towards the NO_2 gas, it is necessary to explain the relation between sensitivity (S) and resistance (R) of the sensor (nanocomposites) [16], when the flow rate of the gas was (80-100 ppm) that has been observed two different resistances when presence the gas and absence [19]. from that different we can get the sensitivity according to following relation [20]:

$$S\% = (R_{\text{on}} - R_{\text{off}}) / (R_{\text{on}}) \times 100 \% \quad \text{..... (1)}$$

While the other important factors in data are response and recovery times [21]. We can define response time as the time to reach a 90% maximum value of conductance (when using reducing gas) or minimum value of conductance (when using oxidizing gas) [22]. on the other hand, the recovery time is the time required to recover within 10% of the original baseline [22] when the flow of reducing or oxidizing gas is removed [23] and according to the definitions,

the data of the three nanocomposites (as sensors) for four different temperatures were compared them as shown in the following tables and figures:

The data sensing

TiO₂/GO nanocomposite of NO₂ sensing as shown in Figure 12

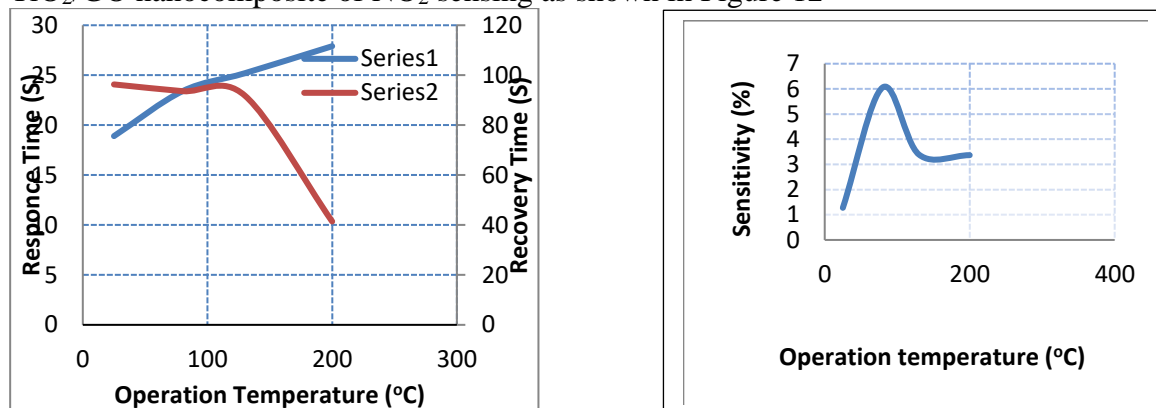


Figure 12: Sensing plots of TiO₂/GO composite.

to summarize the data of TiO₂/GO nanocomposite (sensor) for the different temperatures (25,80,130 and 200 °C) as the following table:

Table 1: The data of TiO₂/GO nanocomposite for NO₂ sensing

No.	Temperature(°C)	Sensitivity (S%)	Response time (sec.)	Recovery time (sec.)
1	25	1.276	18.9	96.3
2	80	6.059	23.4	93.6
3	130	3.391	25.2	91.8
4	200	3.366	27.9	41.4

TiO₂-Ag/GO nanocomposite of NO₂ sensing as shown in Figure 13

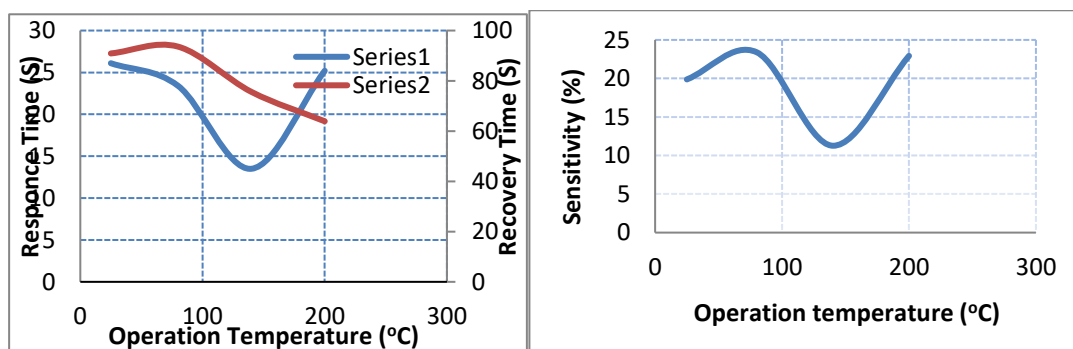


Figure 13: Sensing plots of TiO₂-Ag/GO composite.

Table 2: The data of TiO₂-Ag/GO nanocomposite of NO₂ sensing .

No.	Temperature (°C)	Sensitivity (S%)	Response time (sec.)	Recovery time (sec.)
1	25	19.874	26.1	90.9
2	80	23.399	23.4	93.6
3	130	11.269	13.5	75.6
4	200	22.926	25.2	63.9

TiO₂-Al₂O₃/GO nanocomposite of NO₂ sensing as shown in Figure 14

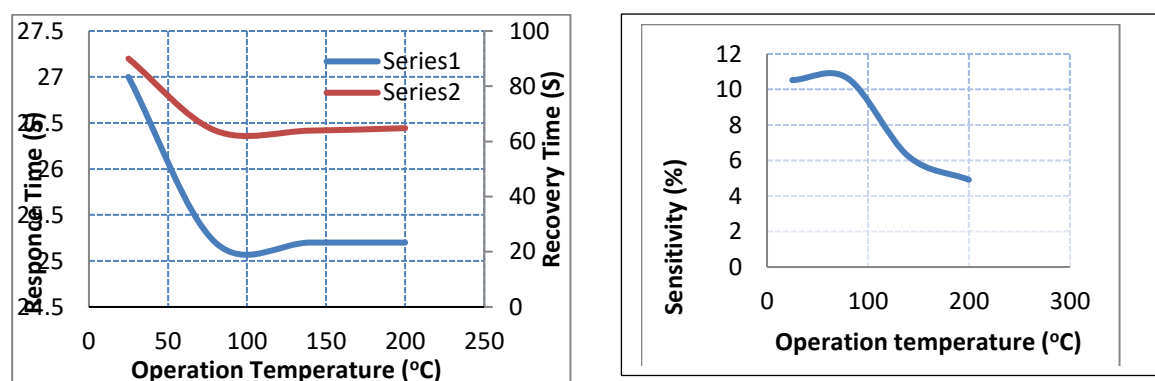


Figure 14: Sensing plots of TiO₂-Al₂O₃/GO composite.

Table 3: The data of TiO₂-Al₂O₃/GO nanocomposite for NO₂ sensing

No.	Temperature (°C)	Sensitivity (S%)	Response time (sec.)	Recovery time (sec.)
1	25	10.526	27.0	90.0
2	80	10.621	25.2	63.9
3	130	6.236	25.2	63.9
4	200	4.915	25.2	64.8

4. Conclusion

The objective of this investigation was to evaluate the gas sensing abilities of three different types of nanocomposites and to assess the impact of additives used in conjunction with the TiO₂/GO nanocomposite. As the results indicate, there was a noticeable variation in sensitivity among the three types of nanocomposites. Moreover, the impact of additives, such as silver - which has the highest electrical conductivity of all metals - and alumina - which boasts strong electroactivity and increases the sensor's surface area [24, 25] - was examined. The addition of these additives led to an increased likelihood of redox reactions between the sensor and NO₂ gas [26], thereby enhancing the sensitivity of the sensor when compared to the TiO₂/GO nanocomposite alone. These findings highlight a potential means of improving sensor performance.

Acknowledgements

I would like to thank Department of chemistry, College of science, University of Baghdad and Dr. Fwad Tariq Ibrahim, Department of physics for their helping to performance this research.

References

- [1] Zaid Hameed Mahmoud, Omar Dhaa Abdalstar and Noor Sabah: "Semiconductor Metal Oxide Nanoparticles: A Review for the Potential of H₂S Gas Sensor Application", *Earthline Journal of Chemical Sciences*, vol. 4, no. 2, pp.199-208, 2020.
- [2] Ali Saad Elewi, Shatha Abdul Wadood Al-Shammaree, Abdul Kareem M.A. AL Sammarraie, "Hydrogen peroxide biosensor based on hemoglobin-modified gold nanoparticles–screen printed carbon electrode", *Sensing and Bio-Sensing Research*, vol. 28, pp.100340, 2020.
- [3] R. Alves Junior, H. P. A. Alves, J. M. Cartaxo, A. M. Rodrigues, G. A. Neves, R. R. Menezes, "Use of nanostructured and modified TiO₂ as a gas sensing agent", *Cerâmica* vol. 67 , no. 383, pp. 316-326, 2021.
- [4] Ghazi M. Abed, Basim I. Al-Abdaly , Abdulkareem M. A. Alsammarraie, "Low

- Temperature Hydrothermal Synthesis of Cu-Nd Doped Zinc Oxide Nanorods", *Iraqi Journal of Science*, Special Issue, Part A, pp:1-10, 2016.
- [5] Ayah F.S. Abu-Hani a, Falah Awwad a, Yaser E. Greish b, Ahmad I. Ayesh c, Saleh T. Mahmoud, Design, fabrication, and characterization of low-power gas sensors based on organic-inorganic nano-composite", *Organic Electronics*, vol. 42 , pp.284-292, 2017.
- [6] Tadeusz Pisarkiewicz , Wojciech Maziarz , Artur Małolepszy , Leszek Stobiński , Dagmara Michoń and Artur Rydosz, "Multilayer Structure of Reduced Graphene Oxide and Copper Oxide as a Gas Sensor" *Coatings*, vol. 10, no. 11, pp. 1015. 2020.
- [7] Junhui Xu & Yazhen Wang & Shengshui Hu, "Nanocomposites of graphene and graphene oxides: Synthesis, molecular functionalization and application in electrochemical sensors and biosensors", A review: *Microchim Acta*, vol. 184, no. 1, pp. 44, 2017.
- [8] Ajeet Kaushik, Rajesh Kumar, Sunil K. Arya, Madhavan Nair, B. D. Malhotra, and Shekhar Bhansali, "Organic-Inorganic Hybrid Nanocomposite-Based Gas Sensors for Environmental Monitoring", *Chem. Rev.* vol. 115, no. 11, pp. 4571–4606, 2015.
- [9] Zakrzewska, K., Radecka, M, "TiO₂-Based Nanomaterials for Gas Sensing—Influence of Anatase and Rutile Contributions", *Nanoscale Res Lett*, vol. 12, no. 89, 2017.
- [10] Sarmed Salih Al-Awadi, AmerA Ramadhan, Fuad T Ibrahim, Ali K Abbood , "Optical and Structural Properties of Titanium Dioxide Papered by DC Magneto-Sputtering as a NO₂ Gas Sensor", *Iraqi Journal of Science*, vol. 61, no. 10, pp. 2562-2569, 2020.
- [11] Burak Yahya Kadem ,R and Kareem Husein,Zahraa Yassar Abbas, "Copper Phthalocyanine MWCNTs Composites: Characterization and Evaluation for Sensor and Solar Cells interlayer", *Iraqi Journal of Science*, vol. 63, no. 8, pp. 3373-3381, 2022.
- [12] Ruqayah A. Ulwali, Heba Kh. Abbas, Ali J Karam , Ali A. Al-Zuky, Mahasin F. Hadi Al-Kadhemy, Anwar H. Al-Saleh, "Surface Plasmon Resonance (SPR) Simulation of a Gold-Bismuth Bi-layer Gas Sensor", *Iraqi Journal of Science*, vol. 63, no. 8, pp. 3402-3411, 2022.
- [13] Riad H. Rakib, Prof. Mohammad A. Hasnat, Prof. Md. Nizam Uddin, M M Alam, Prof. Abdullah M. Asiri, Prof. Mohammed M. Rahman, Prof. Iqbal Ahmed Siddiquey, "Fabrication of a 3,4-Diaminotoluene Sensor Based on a TiO₂-Al₂O₃ Nanocomposite Synthesized by a Fast and Facile Microwave Irradiation Method", *European chemical sciences publishing*, vol. 4, no. 43, pp. 12592-12600, 2019.
- [14] Sanaz, N.; Hamid, R.; Mohammad, F.; Mhammad, S.; Morteza, M, "Mortality response of folate receptor-activated, PEG-functionalized TiO₂ nanoparticles for doxorubicin loading with and without ultraviolet irradiation", *Ceram. Int.*, vol. 40, pp. 5481– 5488, 2014.
- [15] Marta Nycz , Katarzyna Arkusz and Dorota G. Pijanowska, "Fabrication of Electrochemical Biosensor Based on Titanium Dioxide Nanotubes and Silver Nanoparticles for Heat Shock Protein 70 Detection", *Materials*, vol. 14, no. 13, pp. 3767, 2021.
- [16] Sha, H., Zheng, W., Shi, F., Wang, X. and Sun, W., "Direct electrochemistry of hemoglobin on electrodeposited three-dimensional interconnected graphene-silver nanocomposite modified electrode", *Int. J. Electrochem. Sci.*, vol. 11, no. 11, pp. 9656-9665, 2016.
- [17] Dalya jasim Ahmed, Basim Ibrahim Al-abdaly, "Effect of SiO₂ Addition and Calcination Temperature on Surface Area, Crystal Size, Particles Size and Phase Transformation of TiO₂ Prepared by Sol-Gel Method", *Solid State Technology*, vol.64, pp.2, 2021.
- [18] Devanand, G.; Ramasamy, S.; Ramakrishnan, B.; Kumar, J., "Folate targeted PEGylated titanium dioxide nanoparticles as a nanocarrier for targeted paclitaxel drug delivery", *Adv. Powder Technol.*, vol. 24, pp. 947–954, 2013.
- [19] Al-Husseini, A. H., Saleh, W. R., & Al-Sammarraie, A., "A Specific NH₃ Gas Sensor of a Thick MWCNTs-OH Network for Detection at Room Temperature", *Journal of Nano Research*, vol. 56, pp. 98-108. 2019.
- [20] Chetan Kamble, Sandesh Narwade, Rajaram Man, "Detection of acetylene (C₂H₂) gas using Ag-modified ZnO/GO nanorods prepared by a hydrothermal synthesis,

- Materials Science in Semiconductor Processing*", vol. 153, pp. 107145, 2023.
- [21] Nelson Pynadathu Rumjit, Paul Thomas, Chin Wei Lai and Yew Hoong Wong, "Review—Recent Advancements of ZnO/rGO Nanocomposites (NCs) for Electrochemical Gas Sensor Applications", *J. Electrochem. Soc.*, vol. 168, pp. 027506, 2021.
- [22] Nguyen Van Hieu, Phung Thi Hong Van, Le Tien Nhan, Nguyen Van Duy, and Nguyen Duc Hoa, "Giant enhancement of H₂S gas response by decorating n-type SnO₂ nanowires with p-type NiO nanoparticles", *Applied Physics Letters*, vol. 101, pp. 253106, 2012.
- [23] M. Beaula Ruby Kamalam , S.S.R. Inbanathan , B. Renganathan , K. Sethuraman, Enhanced sensing of ethanol gas using fiber optics sensor by hydrothermally synthesized GO-WO₃nanocomposites, *Materials Science and Engineering:B*, vol. 263, pp.114843, 2021.
- [24] A. Ashery, A E H Gaballah and Emad M Ahmed, "Novel negative capacitance, conductance at high and low frequencies in Au/ Polypyrrole–MWCNT composite /TiO₂/Al₂O₃/n-Si structure", *Mater. Res. Express*, vol. 8, pp. 075003, 2021.
- [25] Thamir A.A. Hassan1 , Abdul Kareem M. A. Al-Sammarraie, "Growth of Different Zinc Oxide Nanostructures for Hydrogen Gas Sensing", *Journal of Global Pharma Technology*, vol. 11, no. 02, pp. 419-425, 2019.
- [26] Prashant Bhimrao Koli , Minakshi Dilip Birari , Satish Arvind Ahire , Sachin Girdhar Shinde , Raju Shivaji Ingale , Ishwar Jadhav Patil, "Ferroso-ferric oxide (Fe₃O₄) embedded g-C₃N₄ nanocomposite sensor fabricated by photolithographic technique for environmental pollutant gas sensing and relative humidity characteristics", *Inorganic Chemistry Communications*, vol. 146, pp. 110083, 2022.